

RSC Advances

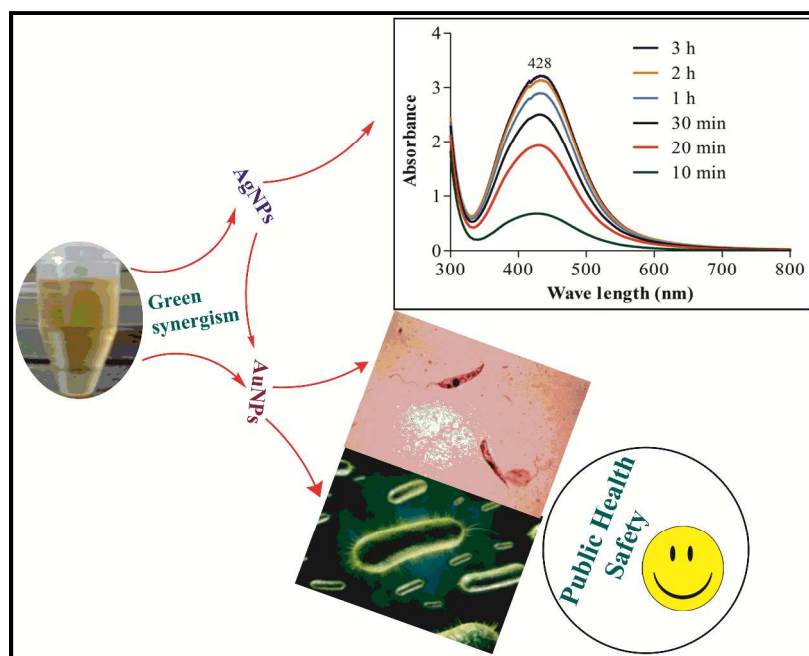


This is an *Accepted Manuscript*, which has been through the Royal Society of Chemistry peer review process and has been accepted for publication.

Accepted Manuscripts are published online shortly after acceptance, before technical editing, formatting and proof reading. Using this free service, authors can make their results available to the community, in citable form, before we publish the edited article. This *Accepted Manuscript* will be replaced by the edited, formatted and paginated article as soon as this is available.

You can find more information about *Accepted Manuscripts* in the [Information for Authors](#).

Please note that technical editing may introduce minor changes to the text and/or graphics, which may alter content. The journal's standard [Terms & Conditions](#) and the [Ethical guidelines](#) still apply. In no event shall the Royal Society of Chemistry be held responsible for any errors or omissions in this *Accepted Manuscript* or any consequences arising from the use of any information it contains.



Graphical abstract

- Promising antileishmanial properties were observed with *Sargentodoxa cuneata* mediated Ag and AuNPs. This study opens a platform for the synthesis new leishmanicidal agents

**Silver and gold nanoparticles from *Sargentodoxa cuneata*: synthesis,
characterization and antileishmanial activities**

Aftab Ahmad^a, *Fatima Syed*^b, *Akram Shah*^c, *Zahid Khan*^b, *Kamran Tahir*^a, *Arif Ullah*

Khan^a, *Qipeng Yuan*^{a*}

^a *State Key Laboratory of Chemical Resource Engineering, Beijing University of Chemical Technology, No. 15 East Road of North Third Ring, Chao Yang District, Beijing 100029, China*

^b *Institute of Chemical Sciences, Biochemistry Section, University of Peshawar (25120) Pakistan*

^c *Department of Zoology, University of Peshawar (25120) Pakistan*

*Authors to whom correspondence should be addressed;

yuanqp@mail.buct.edu.cn, aftabbiochem@yahoo.com ,

Ph: +86 10 64437610 , Fax: +86 10 64437610

Abstract

Leishmaniasis remains one of the fatal diseases worldwide and the conventional antileishmanial therapies are associated with several drawbacks. Therefore, there is a need to develop new antileishmanial strategies. Biogenic silver and gold nanoparticles possess broad-spectrum antimicrobial activities and could be future alternative to current antimicrobial agents. In this report, we present a simple and green approach to synthesize silver and gold nanoparticles with efficient biological activities. Phytochemicals from *Sargentodoxa cuneata* were used to reduce and stabilize the silver and gold ions into metallic nanoparticles. The synthesized nanoparticles were characterized by UV-visible spectroscopy (surface plasmon resonance), X-ray diffraction analysis (crystallinity), High-resolution transmission electron microscopy (size and morphology), energy dispersive X-ray (elemental composition) and FTIR (surface functionalities). Under the optimized conditions, the synthesized silver nanoparticles were spherical in shape, small size (3-8 nm) and well dispersed. However, the gold nanoparticles were mostly hexagonal in shapes with approximate size from 15 to 30 nm. Promising antileishmanial activity was shown by silver and gold nanoparticles with an IC₅₀ value of 4.37 and 5.29 µg/mL respectively. Silver nanoparticles also exhibited significant antibacterial activity against *Staphylococcus aureus* (32 ± 3 mm), *Pseudomonas aeruginosa* (16 ± 2 mm), and *Bacillus subtilis* (18 ± 2 mm). The depicted biological activities of nanoparticles are not simply due to the capped silver and gold atoms but also to their surface macromolecules. Thus, the use of *Sargentodoxa cuneata* as reducing and capping agent will retain its biological activities even after the depletion of maintained silver and gold. The findings of this study indicate that, these nanoparticles could be an alternative, safe, and effective source of antileishmanial agents.

Keyword: *Sargentodoxa cuneata*, silver gold nanoparticles, *Leishmania tropica*, bacteria, antimicrobial activities

1. Introduction

Leishmaniasis is a tropical disease caused by parasites of the genus *Leishmania*. The disease is transmitted by the bite of a female phlebotomine sand fly and has several clinical symptoms that range from self-healing cutaneous to fatal visceral form. World health organization (WHO) has declared leishmaniasis as category 1 disease (most emerging and uncontrollable) affecting approximately 88 countries with annual incidence of cutaneous leishmaniasis around 1.5 million worldwide. The visceral form of leishmaniasis is endemic in the south East Asian region with 300,000 cases in 2006¹. Furthermore, an increase rate of leishmaniasis has been reported around the globe, which has been associated with a possible increase of the disease vectors due to global warming². Severe toxicity and resistance to the current antileishmanial drugs has also been observed in these parasites³. Therefore, an urgent need exists to search for more effective and selective therapeutic agents with broad-spectrum antimicrobial activities. Screening of medicinal plants for the synthesis of metal nanostructures could be a natural alternative for the discovery of new, more effective, less toxic and economical antileishmanial agents.

Nanobiotechnology is an emerging field that is dedicated to create and improve the utility of nanoscale materials for a wide range of applications in advanced biotechnology⁴. These nanostructures have unique characteristic features that arise from their extremely small sizes and large surface area, which are significantly different from those of bulk masses^{5, 6}. The nano forms of silver and gold metals are of special interest in various disciplines, including catalysis, disease diagnoses, gene expression, household consumable products, pharmaceuticals, and cosmetics^{7, 8}. Gold nanocrystals have been used in immunoassay, cancer cells detection, protein

assay, and capillary electrophoresis⁹⁻¹². These nanostructures upon cellular uptake behave as thermal scalpels to kill the infected cell^{13,14}.

Silver is a promising agent possessing broad spectrum antibacterial activity with minimum chance of bacterial resistance to it¹⁵. It has been published that silver ions interfere with bacterial DNA replication, disrupt cell membrane, inhibit critically important enzymes and damage bacteria by a process called respiratory burst mechanism¹⁶⁻¹⁸. Furthermore, silver and gold nanoparticles have the ability to produce reactive oxygen species (ROS), which play an important role in killing pathogenic microbes. It has been reported that leishmania parasites are highly sensitive to ROS¹⁹. In order to kill leishmania parasite by a treatment that involve reactive species, a continuous supply of these oxygen species can be ensured with the use of noble metal nanoparticles. Moreover, small amount of metal nanoparticles are not toxic to human cells and therefore, could be an alternative, safe, and environmentally acceptable antimicrobial agent.

Several physical and chemical methods have been employed to synthesize nanoparticles; however, all those methods are associated with several shortcomings such as the use of toxic chemicals and intensive energy and capital consumption; thus making these synthesis procedures economically expensive and environmentally not friendly. The synthesis of nanoparticles with phytochemicals is a greener, non-toxic, and environmentally acceptable procedure. Plant kingdom represents a renewable source of biologically active phytochemicals, which could be successfully utilized for the synthesis of metal nanoparticles²⁰. The biomolecules of plants may act as both reducing and stabilizing agents in the synthesis of metal nanoparticles^{21,22}.

The use of medicinal plants for the synthesis of nanoscale materials will effectively enhance their biological activities and would remain active even after the depletion of the capped metal.

In the present study, we report on the biogenic synthesis of Ag and Au nanoparticles using phytochemicals from a Chinese medicinal plant "*Sargentodoxa cuneata*". To the best of our knowledge, this is the first report describing the antileishmanial activities of biogenic gold and silver nanoparticles. The prepared Ag and Au nanoparticles were also evaluated for the antibacterial activities.

2. Experimental section

2.1. Preparation of plant extract

Powdered plant material (10 g) was extracted in 200 mL de-ionized water. The suspended plant material was initially heated at 60 °C for 10 min to avoid any possible degradation of the active biomolecules. The suspension was then stirred for 1 h at room temperature (24 °C). The extracted biomass was centrifuged at 5,000 rpm for 5 min to remove the bulk plant material. Finally, the supernatant obtained was filtered through Whatman no.1 filter paper. The clear extract obtained was used for the synthesis of nanoparticles.

2.2. Extraction of phenolic compounds

Dried and finely ground plant material (5 g) was extracted twice with 100 mL aqueous (70%) acetone²³. The suspended plant material in aqueous acetone was subjected to ultrasonic treatment for 20 min at room temperature. The extracted biomass was then filtered and centrifuged (4 °C) at 5000 rpm for 10 min. The supernatant obtained was used as a source of total phenolic contents. Tannin was precipitated from the aqueous extract of *Sargentodoxa cuneata* with polyvinyl polypyrrolidone (PVPP). Both the aqueous extracts after total phenolic and tannin extraction were separately used for the synthesis of silver nanoparticles.

2.3. Synthesis of silver and gold nanoparticles

Silver and gold nanoparticles were synthesized employing the aqueous extract of *Sargentodoxa cuneata* as a reducing and stabilizing agent. To synthesize silver and gold nanoparticles, different concentrations of the plant extract (1-10 mL) were mixed separately with 30 mL of silver nitrate and HAuCl₄.4H₂O (2 mM) solutions. The synthesis procedure was carried out at 30 °C under vigorous stirring. The progress of synthesis was examined by visual observation of the color change from light yellow to deep brown for silver and purplish for gold nanoparticles. At the end of the process, the colloidal suspensions were centrifuged at 10,000 rpm for 10 min. The pellets obtained were washed thrice with distilled water, followed by freeze-drying under vacuum and were finally stored at 4 °C for further use. One of the problems associated with the biogenic synthesis of metal nanoparticles is their reproducibility. In order to address this problem, we performed the biosynthesis of nanoparticles in triplicate under the same experimental conditions. In another experiment, silver nanoparticles were also synthesized by chemical method using NaBH₄ as reducing agent and sodium citrate as capping agent.

2.4. Optimization of nanoparticles synthesis

Various parameters that affect the synthesis of nanoparticles were optimized to get optimal product. The study parameters involved in the optimization process were extract concentration (1-10 mL), metal ions concentration (1-4 mM), pH (4-10), temperature (25-70 °C) and reaction time (0-300 min). The optical density of colloidal suspensions was measured at 428 and 536 nm for silver and gold nanoparticles respectively.

Characterization of nanoparticles

2.5. UV visible spectroscopy

UV-visible spectroscopy was used to monitor the rate of metal reduction and progress of nanoparticles biosynthesis. Aliquots taken from the reaction mixture were scanned at wavelengths between 200 to 800 nm (UV spectrophotometer Shimadzu Japan- 2450).

2.6. High resolution transmission electron microscopy (HRTEM)

High-resolution transmission electron microscope (JEOL-JEM 3010 transmission electron microscope) was used to study the surface morphology, size, and dispersities of the synthesized nanoparticles. Samples for HRTEM were prepared by dissolving 2 mg (sonication) of the nanoparticles in 10 mL methanol. Two drops of the prepared solution were placed on the carbon supported copper grids and were allowed to evaporate the solvent. Particle size distribution was determined from a histogram considering more than 300 particles measured using multiple TEM micrographs.

2.7. XRD analysis

X-ray diffraction analysis was used to determine the crystalline nature and average particles size of the synthesized particles. XRD analysis was performed at 2θ in the range of 20 to 80 degrees using powder X-ray diffractometer (D8 Advance diffractometer).

2.8. Antibacterial assay

The antibacterial activity of the synthesized nanoparticles was tested against four bacterial strains viz *E. coli*, *staphylococcus aureus*, *Pseudomonas aruginosis* and *Bacillus subtilis*. Nutrient agar was autoclaved at 121 °C for 1 h and poured into sterilized Petri plates. The autoclaved agar plates were inoculated with bacterial cells suspension. Wells (6mm) were made in each agar plate using sterile metallic borer. The colloidal suspension of nanoparticles in DMSO was used as test sample while streptomycin and DMSO were used as positive and negative control respectively. In order to assess the antibacterial activity of capped biomolecules, we performed a control experiment with chemically synthesized silver nanoparticles. The plates were incubated at 37 °C for 24 h and the antibacterial activity of the selected nanoparticles was measured as zone of inhibition in mm.

2.9. Antileishmanial activity

Leishmania tropica strain was cultured in medium 199 containing 10% inactivated Fetal Bovine Serum (FBS). The antileishmanial activity was performed according to the procedure described by of Nabi et al. 2012 with slight modification²⁴. The antileishmanial activity of silver and gold nanoparticles was performed against *Leishmania tropica* promastigotes. Every assay tube contained 3 mL of medium with 1×10^5 parasites/mL of *L. tropica* promastigotes. 5 μ L (4 mg/mL) of silver and gold nanoparticles was loaded to each well and incubated at 28 °C. Parasites in both the control and treated samples were counted by hemocytometer at 24, 48, 72 and 96 h of incubation and the activity was expressed as percent inhibition.

2.10. Cytotoxicity assay

The cytotoxicity assay of the phytosynthesized silver nanoparticles was measured using murine macrophages (J774 cell line) by MTT test²⁵. The cells were seeded in 96 well culture plates at a density of 1×10^6 , allowed to attach for 24 h and treated with different concentration (10-1000 μ g/mL) of biosynthesized silver nanoparticles. The treated cells were incubated for 48 h for cytotoxicity analysis. Finally, the cells were subjected to MTT assay. MTT stock concentration (5 mg/mL) was prepared in PBS, and 100 μ L of this solution was added to each wells (AgNPs-treated) and incubated for 4 h. Then, 100 μ L of dimethyl sulphoxide (DMSO) was added to each well (to dissolve the formed purple formazan crystals), and the absorbance values were determined at 590 nm in a multi-well ELISA plate reader (Eliza MAT 2000, DRG Instruments, GmbH). Results were expressed as % cell viability.

$$\% \text{ viability} = \frac{\text{Mean OD of treated samples}}{\text{Mean OD of control sample}} \times 100$$

3. Results and discussion

3.1. UV visible spectroscopy

Formation of silver and gold nanoparticles was confirmed by using UV-Vis spectral analysis. The reduction of gold and silver ions into metallic nanoparticles show a characteristic localized surface plasmon resonance (LSPR), where metal electrons in the conduction band collectively oscillate in resonance upon interaction with light of specific wavelength²⁶. Localized surface plasmon resonance varies with particle size, shape and the reaction medium. The appearance of such characteristic LSPR bands is used to detect the synthesis of metal nanoparticles. Fig.1 illustrates the time dependent evolution of UV-Vis spectra of silver and gold nanoparticles under different experimental conditions. The formation of nanoparticles was controlled by varying the amount of plant extract and metal salts concentration. Initially, the formation of nanoparticles was carried out at 3 mM silver, 2 mM gold and 5 mL plant extract (pH = 7, 30 °C). It was observed that AgNPs revealed a localized-SPR peak of low intensity at 436 nm when 2 mL of the plant extract was mixed with 30 mL (3 mM) silver nitrate solution (Fig 1 a), indicating the synthesis of small amount of nanoparticles. However, when 10 mL of the plant extract was used, the SPR peak blue shifted from 436 to 432 nm with the corresponding increase in peak intensity. This combine phenomenon indicates a faster rate of silver reduction with a narrow size particles distribution (Fig. 1b). The intensity of localized-SPR peak is directly proportional to the concentration of nanoparticles in the solution. However, a red shift in the LSPR pattern (from 432 to 450 nm) was noted with further increase in the aqueous extract (10 mL) of *Sargentodoxa cuneata* (Fig 1 c), suggesting a possible increase in the particle size. Similar variation in the LSPR pattern was also shown by gold nanoparticles synthesized under different plant concentrations. LSPR peaks red shifted from 536 to 562 nm when plant concentration was increased from 5 mL to 10 mL (Fig 1 e, f), suggesting the probability of increasing particle size. An increase in particle size induces a red shift of LSPR from shorter to longer wavelength, which

is in agreement with the HRTEM results (Fig. 4). High concentration of the plant extract introduces more reducing agents, which result a secondary reduction process on the surface of preformed nuclei and additional interaction between the surface biomolecules. The two phenomena giving rise to bigger particles.

The rate of gold reduction was much faster than silver ions, as was observed from the abrupt color change and rapid saturation of peak intensity in 20 min. This is due to the fact that standard reduction potential of Au^{3+}/Au is higher than Ag^+/Ag ²⁷. Furthermore, no detectible change in the peak intensity and blue/red shift pattern was observed after 20 min of incubation, suggesting a nano size distribution of gold nanoparticles and completion of the reaction. The observed uniform symmetry of LSPR bands (Fig. 1) indicates the mono-dispersion of nanoparticles²⁸.

Different concentrations of silver and gold ions were used to get the optimum level of these metals. Both the metals at their low precursor concentrations showed localized-SPR bands with relatively low intensities. However, maximum absorbance was observed for silver and gold nanoparticles at 432 and 536 nm when 3 and 2 mM of silver and gold salts were used (Fig. 1 b,f). Further increase in the salts concentrations resulted visible precipitation with corresponding decrease in absorbance (428 nm) and red shift in the LSPR pattern (Fig.2 b, d). Our results indicated that better size control and maximum production of silver and gold nanoparticles could be achieved at 3 mM AgNO_3 and 2 mM $\text{AuHCl}_4 \cdot 4\text{H}_2\text{O}$ respectively. Similarly, plant extract concentration was optimized by keeping the silver and gold concentration at their constant levels (3 and 2 mM). Results shows that 5 mL of the plant extract demonstrated the best result out of the tested concentrations. Subsequent optimizations of other parameters were carried out by keeping the plant and salt concentrations at their optimum levels. Fig. 3 a represents the effect of pH on the biosynthesis of Ag and AuNPs. Results showed that pH of the reaction media have

strong influence on the biosynthesis of nanoparticles. In both the cases, alkaline pH favored the synthesis of nanoparticles. In the case of silver nanoparticles, alkaline pH resulted an increase in the LSPR peak intensity along with a blue shift, indicating a significant reduction of the silver ions in metallic nanoparticles (Fig. 1d). Previous study reveals that silver ions are efficiently reduced at higher pH²⁹. This observation suggests that higher pH induces more nucleation and growth of metal nanoparticles, which may be due to the activation of the phytochemicals involved in their synthesis in alkaline conditions. Kajani *et al.* also reported that alkaline pH is suitable for the synthesis of silver and gold nanoparticles²¹.

The effect of reaction temperature on the biogenic synthesis of gold and silver nanoparticles is shown in Fig. 3 b. A gradual increase in the absorbance at 428 and 536 nm was noted for both silver and gold nanoparticles, indicating that metal reduction is accelerated in the presence of plant extract at elevated temperature. However, it was observed that a slight decrease in the SPR band intensity occurred beyond 50 °C in the cases of gold and 60 °C in the case of silver nanoparticles. This indicates reaction saturation and may presents a tendency for precipitation at elevated temperature.

The progress of nanoparticles synthesis was monitored for 300 min. The rate of silver reduction was relatively slow and maximum localized SPR intensity was observed after 180 min (Fig. 3 c). On the other hand, the rate of gold reduction was faster than silver ions as evident from the appearance of maximum LSPR intensity within 20 min. No major increase in the LSPR intensity was observed after 20 minutes indicating the completion of reaction. Under the optimized conditions (5 mL extract, 3 mM silver, 60 °C and pH 8), the prepared silver nanoparticles revealed maximum SPR intensity (Fig.1d). Similarly, gold nanoparticles shoed maximum SPR peak at 5 mL extract, 2 mM gold solution, 50 °C and pH 8 (Fig 1 i).

The stem extract of *Sargentodoxa cuneata* is rich in various phytochemicals like phenolic compounds and flavonoids. These phytochemicals play an important role in the synthesis of nanoparticles by reducing and stabilizing the metal ions into metallic nanoparticles. The surface adhered biomolecules form a covering on the nanoparticles and hence protect them from aggregation.

3.2. XRD analysis

XRD pattern of the synthesized nanoparticles (Fig. 4) indicates four diffraction bands at 38.175°, 44.093°, 64.431° and 77.373° which can be attributed to (1 1 1), (2 0 0), (2 2 0) and (3 1 1) Bragg reflection pattern of the face centered cubic structure of metallic silver (reference file JCPDS no. 04-0783). As evident from the observed pattern, the most significant peak is centered at $2\theta = 38.175^\circ$, which is originated from the face centered cubic silver³⁰. This result clearly shows that the top crystal plane (basal plane) of the synthesized nanoparticles must be the (111) plane. Similar diffraction patterns have been previously reported for silver and gold nanoparticles using plant extract as reducing and capping agents³¹. When compared the broadness of XRD peaks for silver and gold nanostructures, it is seen (Fig. 4) that XRD peaks are much broader for silver nanoparticles as compared to gold NPs, suggesting a smaller size distribution for silver relative to gold nanoparticles. The silver nanoparticles with smaller size have wider peaks (Fig 4 A-ii) as compare to their larger counterparts (Fig 4 A-i). This pattern is also supported by the result obtained from high resolution TEM. Similarly, the XRD pattern of gold nanoparticles with different particles size has been given in fig. 4 B.

The average particles size of the synthesized nanoparticles was calculated from the Debye-Scherrer's equation (1)

$$d = \frac{K\lambda}{\beta \cos \theta} \quad (1)$$

Where, d is particle size, K is the Scherer constant with value from 0.9 to 1 (shape factor), λ is the wave length of the X-ray source, β is full width half maxima in radians (FWHM) and θ is the Bragg angle. The sizes of silver and gold nanoparticles (under optimized conditions, 5 mL extract) were about 7 and 25nm respectively. These results were in agreement with the sizes of nanoparticles obtained from the HRTEM study. The calculated d spacing (fringe spacing) between the lattice planes for (111) plane was found to be 0.236 nm, which was in agreement with the lattice spacing of the reference (JCPDS file No. 04-0784d = 0.2359 nm). Similarly, the lattice constant " a " of AgNPs was determined from the following equation (2).

$$a = d_{hkl} \sqrt{(h^2 + k^2 + l^2)} \quad (2)$$

Where " a " is the lattice parameter, d_{hkl} is plane spacing for (111) plane and hkl are the crystallographic dimensions. The lattice parameter for silver nanoparticles (4.08 Å), as calculated from the above equation (equ. 2), was in full agreement with the reference standard 4.086 Å (JCPDS 04-0783).

3.3. EDX analysis

Fig. 5 shows the EDX pattern of Ag and Au nanoparticles. Appearance of strong peak around 3 KeV designate the position of elemental silver which arises from the localized surface plasmon resonance in AgNPs²¹. Similarly, the appearance of strong peak around 2 KeV confirmed the elemental gold as major constituent along with small signals from C, O and Cu atoms in gold nanoparticles. Overall EDX result exhibited the presence of elemental silver and gold as major constituents with small amount of carbon and traces of copper signals. These weak signals may be originated from the surface bound macromolecules and the copper grids used as supporting filament (Cu signal).

3.4. High-resolution transmission electron microscopy (HRTEM)

The biological activities associated with silver and gold nanoparticles are size, shape, and degree of dispersion dependent. These three parameters of the synthesized nanoparticles were determined by transmission electron microscopy (HRTEM) and the result is shown in fig. 6. Different concentrations of the plant extract were used to get the narrow size distribution of nanoparticles. Under the optimized conditions (5 mL extract/30 mL, 2.5 mM gold solution), the synthesized gold nanoparticles were well dispersed, mostly hexagonal in shape with scattered pyramids (Fig. 6a). The biogenic synthesis of gold nanoparticles of mixed shapes has also been previously recorded with plant extracts using 10 mM HAuCl₄ [32]. The approximate particles size was in the range of 20-40 nm. This result is in agreement with particle size calculated from XRD pattern using Scherer's formula (~25 nm). However, when high concentration of the plant extract (10 mL/30 mL, 2.5 mM gold solution) was used, the resulted particles were larger in size (50-80 nm) and were mostly fused together (Fig. 6b). The synthesized silver nanoparticles using 3 mM AgNO₃ and 5 mL plant extract were mostly spherical in shapes with approximate grain size of 5-8 nm (Fig. 6c). The same way, silver nanoparticles synthesized under high plant concentration were larger in size (5-15 nm) with some degree of aggregation (Fig. 6d). It has been previously reported that particle size is directly related to the total phenolic content in the plant extract. Higher concentration of the phenolic content results in larger particle size and our results are in close agreement with the previous findings³³. The observed increase in particle size at higher plant concentration may be due to the elevated level of poly-phenolic contents. These compounds play a critical role in the formation of nanoparticles as previously been reported for other plants³³. It is also important to note that both Ag and AuNPs are surrounded by a thin layer, suggesting that biomolecules present in *Sargentodoxa cuneata* have capped and adhered to the surface of these particles³¹.

3.5. FTIR analysis

FTIR spectrum of AgNPs revealed significant peaks at 3432, 2922, 1628 and 1040 cm^{-1} while several weak bands were also observed at 2852, 1511, 1382 and 1129 cm^{-1} (Fig. 7a). The peak appeared at 3432 is attributed to the O-H stretching frequency of hydroxyl group of phenolic compounds, peaks at 2852 cm^{-1} and 2922 cm^{-1} could be due C-H stretching vibration of methyl or methylene groups [35]. The strong peaks at 1628 cm^{-1} and 1040 cm^{-1} represent the carbonyl group stretching vibration of flavonoids and ester bonds in polyphenolic (tannin) [36] [32, 37]. Other weak peaks around 1500 cm^{-1} and 1129 cm^{-1} correspond to stretching vibration of aromatic -C-C- groups and C-O functional in tannin/tannic acid^{38,39}.

Similar pattern of FTIR spectra was also observed for the gold nanoparticles with the exception of a strong peak at 1021 cm^{-1} (Fig. 7b). This peak corresponds to the ester bonds in phenolic compounds (tannins), suggesting a strong involvement of tannin in the synthesis of gold nanoparticles. The possible phytochemicals of the selected plant such as poly-phenolics such as flavonoids and tannin, as indicated from the FTIR spectra, may be involved in metal reduction and capping for the synthesis of silver and gold nanoparticles^{40,41}.

Polyphenolic compounds (tannins) contain sufficient hydroxyl and other suitable groups (such as carboxyl) to form strong complexes with various metal ions⁴². Tannins are water soluble polyphenols that constitute a major portion (more than 10 % of the dry weight) of higher herbaceous and woody plants, where they play an important role in protection from microbial attack and their colonization⁴³.

Phytochemical analysis of the aqueous extract of *Sargentodoxa cuneata* reveals the presence of flavonoids, tannins, phenolic glycosides, and reducing sugars (Table 1). Previous studies also verify the presence of phenolic glycosides, flavonoids, anthraquinones, and organic acids in the

aqueous extract of *Sargentodoxa cuneata*⁴⁴⁻⁴⁶. Most of the detected compounds in the aqueous extract of *Sargentodoxa cuneata* such as flavonoids, tannins and other phenolic compounds possess strong antibacterial and anti-parasitic activities^{47, 48}.

Based on the FTIR spectral analysis of silver and gold nanoparticles for the surface adhered biomolecules and experimental work, we proposed a mechanism (Fig. 8) for the reduction and capping of metal ions into metal nanoparticles. It is suggested that flavonoids and other phenolic compounds in the plant extract such as tannin may be responsible for the reduction and subsequent stabilization of silver and gold ions. These compounds possess sufficient hydroxyl and carboxyl groups, which are able to bind to metals. The chelating ability of phenolic compounds is possibly related to the strong nucleophilic character of the aromatic rings rather than to specific chelating groups within these molecules⁴⁹.

3.6. Synthesis of AgNPs in the absence of phenolics

When the aqueous extract of *Sargentodoxa cuneata* (after the extraction of polyphenols) was used for the synthesis of silver nanoparticles, it was observed that the rate of metal reduction was very slow as evident from the sluggish color change after 10 h of the reaction. This observation suggests that phenolic compounds in the plant extract are majorly responsible for the reduction of metal ions into metal nanoparticles. The role of tannin as a reductant and stabilizer was also investigated in an experiment when AgNPs were prepared with the aqueous extract after tannin precipitation with polyvinyl polypyrrolidone (PVPP). The LSPR pattern of these nanoparticles was of low intensity with significant red shift, indicating a possible increase in particles size. Furthermore, aggregation and fusion among the particles was also observed, revealing the lack of sufficient capping agent, which could stabilize the metal nanoparticles (Fig. 6 e). These observations suggest that in the absence of tannin in the aqueous extract, the metal nanoparticles

were not fully stabilized and hence resulted aggregation and fusion among them. All these observation suggest that polyphenolic compounds are the main players in the synthesis of metal nanoparticles. Our results are in agreement with previous findings that phenolic compounds are mainly responsible for metal reduction and capping^{32,50}.

3.7. Antibacterial activity

The emergence of new infectious diseases and increased incidence of bacterial resistance is a serious health problem worldwide. There is an urgent need for the discovery of new, safer, and more potent therapeutic agents to treat the emerging microbial resistance and other medical conditions. The potential of a medicinal plant "*Sargentodoxa cuneata*" was exploited in the synthesis of silver and gold nanoparticles to enhance its biological activities. The synthesized nanoparticles were tested against four bacterial strains and the results showed variation with respect to antibacterial response (Table 2). The silver nanoparticles exhibited significant activity against *staphylococcus aureus*, *Pseudomonas araginosis* and *bacillus subtilis* with zone of inhibition 32 ± 2.6 , 16 ± 2 and 18 ± 2 mm respectively, even more potent than the standard drug used (Fig. 9). However, both silver and gold nanoparticles were moderately active against *E. coli* with zone of inhibition 12 ± 1 and 11 ± 1 mm respectively. The strong antibacterial activity of AgNPs (compared to AuNPs) may be attributed to their small size and spherical morphology. Smaller particles sizes with spherical morphology have large surface area for contact with microorganisms, and are therefore more active than their larger counterparts. Furthermore, the surface adhered biomolecules in metal nanoparticles also contribute to the biological activities of these nanostructures. *Sargentodoxa cuneata* mediated silver nanoparticles exhibited strong antibacterial activity against *Klebsiella Pneumoneae* (17 ± 1.4) and *Bacillus subtilis* (16 ± 1.5) in a control experiment as compared to chemically synthesized silver nanoparticles (10 ± 1.2 , 12 ± 1.4 respectively). This result clearly suggests that the improved biological activity of

Sargentodoxa cuneata mediated AgNPs are not simply due to capped silver and gold atoms but also to their surface macromolecules (Fig. 9).

It has been suggested that antibacterial effect is mainly due to silver release from the AgNPs, followed by the interaction of silver ions with the cellular targets^{18, 51}. Silver ions exert their antimicrobial activity by several mechanisms such as (i). Ag ions interact with the thiol group of critically important enzymes and inhibit them (ii). Interfere with the respiratory mechanism (iii). interact with phosphate group in DNA and interfere its ability to replicate (iv) cause K⁺ depletion thus disrupt cellular transport system (v) physical contact of silver nanoparticles disrupt cell membrane and (vi) production of reactive oxygen species from silver ions and silver particles¹⁶⁻¹⁸. Previous findings indicate that control release of silver from nanoparticles induces the production of reactive oxygen species in pathogenic bacteria^{17, 52}. When the levels of these reactive species overcome the scavenging capacity of bacterial cell, they cause damage to bacterial protein and DNA¹⁷. The most important result of the present study is that AgNPs exhibited significant activity against *Pseudomonas aruginosis*, which was resistant to several antibiotics including streptomycin. The *Pseudomonas aruginosis* is usually isolated from the burn wounds, and the AgNPs could be successfully applied to treat the multi-drug resistant bacteria in such medical conditions. Secondly, the AgNPs also showed significant activity (32 ± 3 mm) against a streptomycin resistant *staphylococcus aureus*, making these nanoparticles of significant importance as antibacterial agents.

3.8. Antileishmanial activity

The antileishmanial activity of silver and gold nanoparticles was tested against *Leishmania tropica* as a modal parasite. The efficacy of all the tested nanoparticles was studied for 96 h and the antileishmanial activity was expressed as percent inhibition. To make determinations, the

number of promastigotes was counted in both control and experimental groups at different time intervals (24, 48, 72 and 96 h). It was observed that the number of cells significantly decreased in each group, when compared with the control group, after exposure to silver and gold nanoparticles. Fig. 10 (a, b) shows the time dependent antileishmanial activities of silver and gold nanoparticles. The observed decrease in the parasite count after 24 h of incubation is shown in fig. 10 c. It is obvious from the results that the parasite count significantly decreased in the first 24 h of incubation with the nanoparticles. Ag and Au nanoparticles showed 90 and 62% inhibition within this time period respectively. The number of cells count was further decreased in the treated samples when examined at 48 h of incubation. Both the Ag and Au nanoparticles showed significant activity against the parasite, however, the silver nanoparticles presented an excellent antileishmanial activity with maximum of 95.45 % inhibition at 48 h of incubation. From then onward, AgNPs showed a negligible decline in activity after 48 h of incubation, while an increase in leishmanicidal activity was observed for AuNPs (77.5%).

Several mechanisms have been proposed for the antimicrobial property of metal nanoparticles. A number of reports suggest that the antimicrobial effect relay mainly on the slow release of silver ions from nanoparticles surface, followed by interaction with microbial cell surface, penetration into the cytoplasm and binding with the target sites^{17, 53}. Furthermore, noble metal nanoparticles are able to produce reactive oxygen species, which destroy pathogenic microbes by a process called respiratory burst mechanism. It has been stated earlier that *Leishmania* is highly sensitive to these oxygen species and the drug, which could generate ROS, will be efficient antileishmanial agents. Macrophages (host cells for *Leishmania*) produce high concentration of these ROS to disinfect microbial agents⁵⁴. However, *Leishmania* bypasses the oxidative damage caused by ROS by inhibiting the enzymes that are involved in the process of ROS production⁵⁵.

The use of Ag and Au nanoparticles as leishmanicidal agents will act as a large reservoir of silver and gold ions, which will provide a non-enzymatic source of ROS and will destroy the invaded parasite. Electron spin resonance spectroscopy has confirmed the generation of free radicals from silver ions, and these radicals damage microbial cells by several mechanisms⁵⁶.

Previous studies also indicate that metal containing compounds have promising antileishmanial activities. Gold containing complexes are efficient inhibitors of metabolically important enzymes in *Leishmania*. According to researchers, *Trypanothione reductase* is a critically important enzyme, which controls the polyamine-dependent redox metabolic activity of *Leishmania*, and is therefore an attractive target for designing leishmanicidal drugs. Recent studies have demonstrated that gold containing compounds exert antileishmanial activity by inhibiting *Trypanothione reductase*⁵⁷. *Trypanothione reductase* and *Trypanothione synthetase* are two essential enzymes for Leishmanial survival. These enzymes play an important role in protecting *Leishmania* from the oxidative damage, and allowing the delivery of the reducing equivalents for DNA synthesis. The absence of *Trypanothione reductase* and *Trypanothione synthetase* in mammalian host and the well-known sensitivity of *Leishmania* to ROS make these enzymes as selective target for antileishmanial drugs. Furthermore, gold-based drugs are also efficient inhibitors of *thioredoxin glutathione reductase*, and inhibition of this enzyme upsets the intracellular redox balance, followed by induction of oxidative stress and subsequent cytotoxic effects⁵⁸. The strong antileishmanial activities of our samples may be due to inhibitory effects on some of the metabolically important enzymes.

The corresponding concentrations of *Maytenus* extract were also used to investigate the antileishmanial activity of the aqueous extract leishmania tropica cells as control experiments.

The maximum mortalities of 42.24 % were obtained after 72 hours incubation in the highest concentration of aqueous extracts. This indicates the moderate antileishmanial activity of *Maytenus royleanus* aqueous extract. Concerning the antileishmanial activity of biogenic silver and gold nanoparticles, it can be concluded that the coating of gold and silver nanoparticles with *Maytenus* extract displays synergistic antimicrobial effects. The significant results of our findings thus clearly demonstrate that low concentrations of silver nanoparticles can significantly inhibit *Leishmania* and may be a promising agent for the treatment of leishmaniasis.

3.9. Cytotoxicity of biogenic silver nanoparticles

The development of more effective and less toxic agents are required to treat a particular pathological condition. Silver nanoparticles are strong candidates possessing broad-spectrum antimicrobial activities. However, it is important to evaluate the cytotoxic effects of these nanostructures on normal cells in order to ensure their safe use. The phyto-synthesized silver nanoparticles were evaluated for their effect on cell viability against murine macrophages (J774 cell line) in a dose dependent manner. Results indicated that AgNPs did not show any prominent cytotoxicity at low concentrations and less cytotoxicity was observed at higher concentration above 80 $\mu\text{g/mL}$ (Fig. 11). The biosynthesized AgNPs exhibited 50% cell inhibition (IC_{50}) at 116 $\mu\text{g/mL}$ which is very high than the inhibitory concentration against *leishmania tropica* ($\text{IC}_{50} = 4.37 \mu\text{g/mL}$). Our results also indicate that AgNPs synthesized with *Sargentodoxa cuneata* are less cytotoxic than previously reported biogenic silver and gold nanoparticles⁵⁹⁻⁶¹. Hence, the present investigation suggests that at limited dosage, the *Sargentodoxa cuneata* mediated AgNPs can be used as an effective antileishmanial agent with minimum toxicity.

4. Conclusion

The present contribution demonstrated the synthesis of silver and gold nanoparticles employing an eco-friendly green approach. The aqueous extract of *Sargentodoxa cuneata* was successfully used as reducing and capping agent without any aided supportive chemicals. Subsequent characterization of the synthesized nanoparticles was carried out using UV-visible spectroscopy, XRD, EDX, HRTEM and FTIR techniques. Silver nanoparticles showed significant activity against *Staphylococcus aureus* (32 ± 3), *Pseudomonas araginosis* (16 ± 2) and *Bacillus subtilis* (18 ± 2) while moderate activity was recorded with *E. coli* ($10 \text{ nm} \pm 1.2$). Importantly, the Ag and AuNPs size can be controllably varied by changing the concentration of *Sargentodoxa cuneata* stem extract. The absorption spectra of nanoparticles were tuned, by carefully optimizing various process parameters for the synthesis of small sized nanoparticles.

Promising antileishmanial activity was shown (for promastigotes form) by AgNPs, inhibiting the growth of parasite by 95 %. Gold nanoparticles also presented a significant activity against *Leishmania tropica* at 48 h of incubation ($75\% \pm 14$). The green synthesized silver nanoparticles were shown to have minimum toxicity ($IC_{50} = 116 \mu\text{g/mL}$) against the normal human cells. Thus, this study provides a platform to synthesize more effective and less toxic antimicrobial agents by a green method for use in pharmaceutical industry. Furthermore, the use of silver and gold nanoparticles may represent a future alternative to current antileishmanial drugs. This is the first report on biogenic synthesis of silver and gold nanoparticles using the aqueous extract of *Sargentodoxa cuneata*.

Acknowledgment

The authors are highly grateful to International Science & Technology Cooperation Program of China (Grant No. 2013DFR90290) for supporting the current project.

References

- [1] W.H. Organization, Addis Ababa, Ethiopia, 2007, 20-22.

- [2] A.T. Peterson and J. Shaw, *International journal for parasitology.*, 2003, **33**, 919-931.
- [3] S. Natera, C. Machuca, M. Padrón-Nieves, A. Romero, E. Díaz and A. Ponte-Sucre, *Int. J. Antimicrob. Agents.*, 2007, **29**, 637-642.
- [4] D.S. Goodsell, *Bionanotechnology: lessons from nature*, John Wiley & Sons, 2004.
- [5] M.-C. Daniel and D. Astruc, *Chemical reviews.*, 2004, **104**, 293-346.
- [6] K.M.A. El-Nour, A.a. Eftaiha, A. Al-Warthan and R.A. Ammar, *Arabian journal of chemistry.*, 2010, **3**, 135-140.
- [7] S.A. Aromal and D. Philip, *Spectrochimica Acta Part A: Molecular and Biomolecular Spectroscopy.*, 2012, **97**, 1-5.
- [8] M.S. Akhtar, J. Panwar and Y.S. Yun, *ACS Sustainable Chemistry & Engineering.*, 2013, **1**, 591-602.
- [9] X. Liu, Q. Dai, L. Austin, J. Coutts, G. Knowles, J. Zou, H. Chen and Q. Huo, *J. Am. Chem. Soc.*, 2008, **130**, 2780-2782.
- [10] D. Tang, R. Yuan, Y. Chai, X. Zhong, Y. Liu and J. Dai, *Clin. Biochem.*, 2006, **39**, 309-314.
- [11] C.D. Medley, J.E. Smith, Z. Tang, Y. Wu, S. Bamrungsap and W. Tan, *Anal. Chem.*, 2008, **80**, 1067-1072.
- [12] W.L. Tseng, M.F. Huang, Y.F. Huang and H.T. Chang, *Electrophoresis.*, 2005, **26**, 3069-3075.
- [13] X. Huang, I.H. El-Sayed, W. Qian and M.A. El-Sayed, *J. Am. Chem. Soc.*, 2006, **128**, 2115-2120.
- [14] O.V. Salata, *Journal of nanobiotechnology.*, 2004, **2**, 3.
- [15] J. Morones, J. Elechiguerra and A.H. Camacho, *Nanotechnology.*, 2005, **16**, 2346-2352.

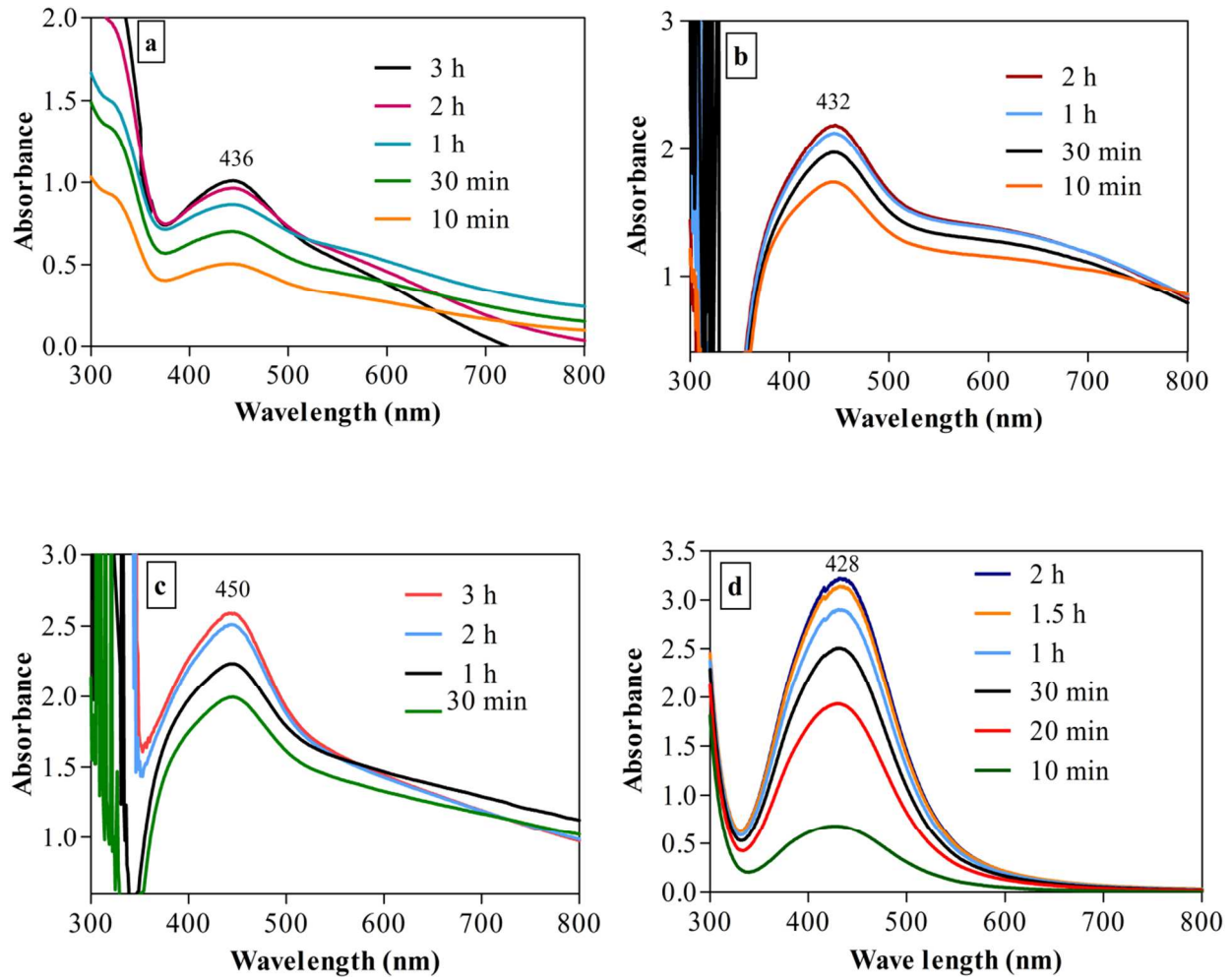
- [16] K. Chamakura, R. Perez-Ballester, Z. Luo, S. Bashir, J. Liu, *Colloids Surf. B. Biointerfaces.*, 2011, **84**, 88-96.
- [17] J.R. Morones, J.L. Elechiguerra, A. Camacho, K. Holt, J.B. Kouri, J.T. Ramírez, M.J. Yacaman, *Nanotechnology.*, 2005, **16**, 2346.
- [18] K.B. Holt and A.J. Bard, *Biochemistry.*, 2005, **44**, 13214-13223.
- [19] H.W. Murray, *The Journal of experimental medicine.*, 1981, **153**, 1302-1315.
- [20] J. Lee, E.Y. Park and J. Lee, *Bioprocess and biosystems engineering.*, 2014, **37**, 983-989.
- [21] A.A. Kajani, A.-K. Bordbar, S.H.Z. Esfahani, A.R. Khosropour and A. Razmjou, *RSC Advances.*, 2014, **4**, 61394-61403.
- [22] C. Krishnaraj, P. Muthukumar, R. Ramachandran, M. Balakumaran and P. Kalaichelvan, *Biotechnology Reports.*, 2014, **4**, 42-49.
- [23] H.P. Makkar, *Quantification of tannins in tree and shrub foliage: a laboratory manual*, Springer Science & Business Media, 2003.
- [24] S. Nabi, N. Ahmed, M.J. Khan, Z. Bazai, M. Yasinzai and Y. Al-Kahraman, *World Applied Sciences Journal.*, 2012, **19**, 1495-1500.
- [25] T. Mosmann, *Journal of immunological methods.*, 1983, **65**, 55-63.
- [26] K.L. Kelly, E. Coronado, L.L. Zhao and G.C. Schatz, *The Journal of Physical Chemistry B.*, 2003, **107**, 668-677.
- [27] N.A. Begum, S. Mondal, S. Basu, R.A. Laskar and D. Mandal, *Colloids Surf. B. Biointerfaces.*, 2009, **71**, 113-118.
- [28] M. Bindhu and M. Umadevi, *Spectrochimica Acta Part A: Molecular and Biomolecular Spectroscopy.*, 2014, **121**, 596-604.

- [29] A.A. AbdelHamid, M.A. Al-Ghobashy, M. Fawzy, M.B. Mohamed and M.M. Abdel-Mottaleb, *ACS Sustainable Chemistry & Engineering.*, 2013, **1**, 1520-1529.
- [30] P.D.D. Files, Pennsylvania, PA (1991).
- [31] M. Nasrollahzadeh, S.M. Sajadi, F. Babaei and M. Maham, *Journal of colloid and interface science.*, 2015, **450**, 374-380.
- [32] V. Reddy, R.S. Torati, S. Oh and C. Kim, *Ind. Eng. Chem. Res.*, 2012, **52**, 556-564.
- [33] V. Kumar, S.C. Yadav, S.K. Yadav and J. Chem. Technol. Biotechnol., 2010, **85**, 1301-1309.
- [34] N. Ahmad, S. Sharma, M.K. Alam, V. Singh, S. Shamsi, B. Mehta and A. Fatma, *Colloids Surf. B. Biointerfaces.*, 2010, **81**, 81-86.
- [35] B.H. Stuart, *Infrared spectroscopy: Fundamentals and applications.*, 2004 71-93.
- [36] H. Ozgunay, O. Sari and M. Tozan, *The Journal of the American Leather Chemists Association.*, 2007, **102**, 154-157.
- [37] J.Y. Song, H.-K. Jang and B.S. Kim, *Process Biochem.*, 2009, **44**, 1133-1138.
- [38] B. Stuart, *Infrared spectroscopy*, Wiley Online Library, 2005.
- [39] M.A. Pantoja-Castro and H. González-Rodríguez, *Revista latinoamericana de química.*, 2011, **39**, 107-112.
- [40] S. Otari, R. Patil, S. Ghosh and S. Pawar, *Mater. Lett.*, 2014, **116**, 367-369.
- [41] R. Sathyavathi, M.B. Krishna, S.V. Rao, R. Saritha and D.N. Rao, *Advanced science letters.*, 2010, **3**, 138-143.
- [42] K.-T. Chung, T.Y. Wong, C.-I. Wei, Y.W. Huang and Y. Lin, *Critical reviews in food science and nutrition.*, 1998, **38** 421-464.
- [43] A. Scalbert, *Phytochemistry* 30 (1991) 3875-3883.

- [44] J. Chang and R. Case, *Phytochemistry.*, 2005, **66**, 2752-2758.
- [45] T. Jian, M. Rui-Li, Z. OUYANG and C. Hai-Sheng, *Chinese Journal of Natural Medicines.*, 2012, **10**, 115-118.
- [46] Y. Tian, H. Zhang, A. Tu, J. Dong and Yao xue xue bao, *Acta pharmaceutica Sinica.*, 2005, **40**, 628-631.
- [47] H. Kolodziej and A.F. Kiderlen, *Phytochemistry.*, 2005, **66**, 2056-2071.
- [48] T.T. Cushnie and A.J. Lamb, *International journal of antimicrobial agents.*, 2005, **26**, 343-356.
- [49] J.B. Harborne, *Biochemistry of phenolic compounds.* (1964).
- [50] J. Das and P. Velusamy, *Journal of the Taiwan Institute of Chemical Engineers.*, 2014, **45**, 2280-2285.
- [51] Q. Feng, J. Wu, G. Chen, F. Cui, T. Kim and J. Kim, *J. Biomed. Mater. Res.*, 2001, 662-668.
- [52] R. Dutta, B.P. Nenavathu, M.K. Gangishetty and A. Reddy, *Colloids Surf. B. Biointerfaces.*, 2012, **94**, 143-150.
- [53] M. Yamanaka, K. Hara and J. Kudo, *Appl. Environ. Microbiol.*, 2005, **71**, 7589-7593.
- [54] R. Lodge and A. Descoteaux, *Eur. J. Immunol.*, 2006, **36**, 2735-2744.
- [55] A. Mehta and C. Shaha, *Free Radic. Biol. Med.*, 2006, **40**, 1857-1868.
- [56] J.S. Kim, E. Kuk, K.N. Yu, J.-H. Kim, S.J. Park, H.J. Lee, S.H. Kim, Y.K. Park, Y.H. Park and C.Y. Hwang, *Nanomed. Nanotechnol. Biol. Med.*, 2007, **3**, 95-101.
- [57] A. Ilari, P. Baiocco, L. Messori, A. Fiorillo, A. Boffi, M. Gramiccia, T. Di Muccio and G. Colotti, *Amino Acids.*, 2012, **42**, 803-811.

- [58] A.N. Kuntz, E. Davioud-Charvet, A.A. Sayed, L.L. Califf, J. Dessolin, E.S. Arnér and D.L. Williams, *PLoS Med.*, 2007, **4**, e206.
- [59] R. Vivek, R. Thangam, K. Muthuchelian, P. Gunasekaran, K. Kaveri and S. Kannan, *Process Biochemistry.*, 2012, **47**, 2405-2410.
- [60] N. Kanipandian, S. Kannan, R. Ramesh, P. Subramanian and R. Thirumurugan, *Materials Research Bulletin.*, 2014, **49**, 494-502.
- [61] P. Manivasagan, M.S. Alam, K.-H. Kang, M. Kwak and S.K. Kim, *Bioprocess and biosystems engineering.*, 2015, **38**, 1167-1177.

Figure 1



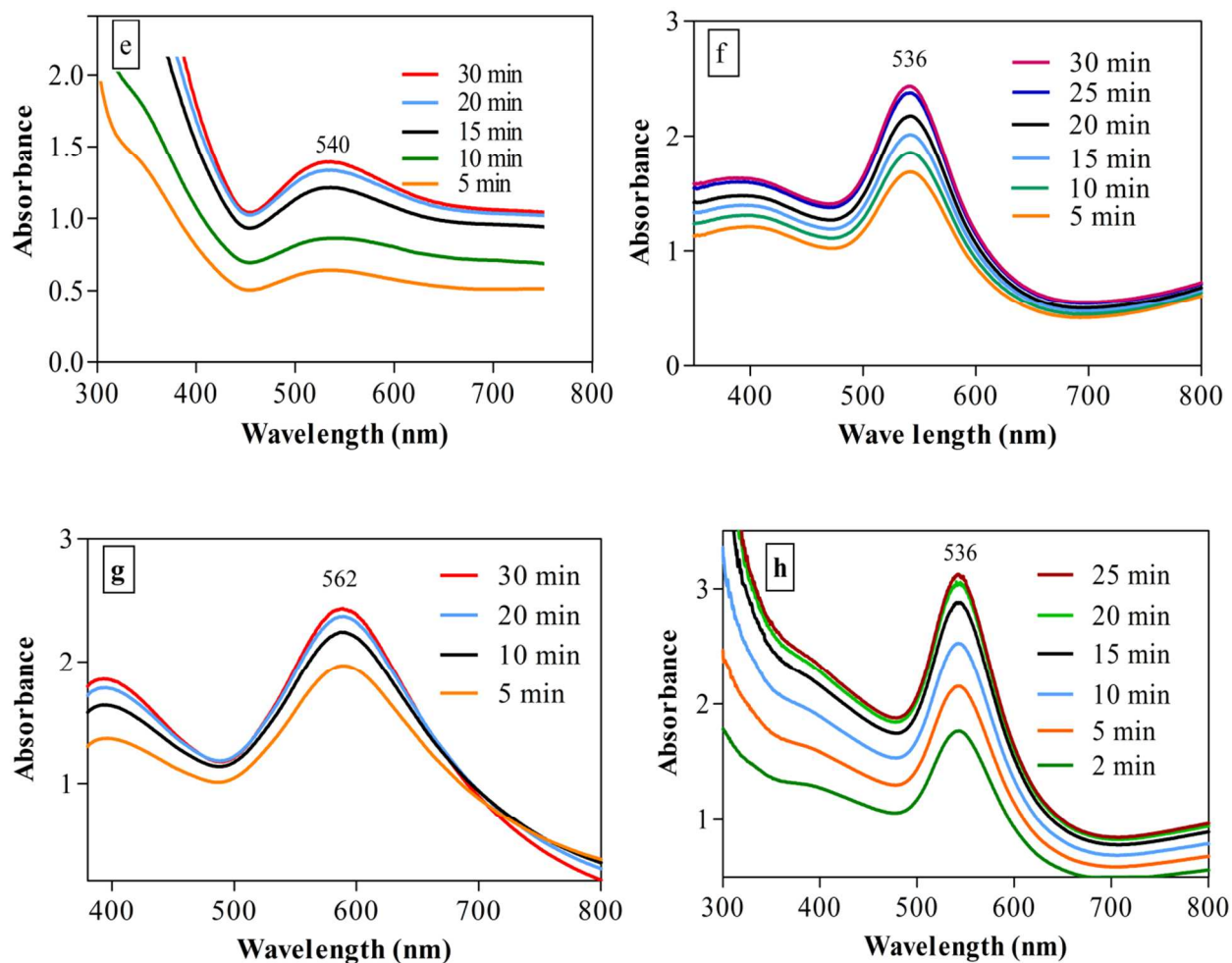


Fig. 1. Time dependent evolution of UV-visible spectra of silver and gold nanoparticles under varying amount (mL) of plant extract at 3 and 2 mM silver and gold ions respectively. (a) 2 mL extract and 3 mM AgNO_3 (b) 5 mL extract (c) 10 mL extract and (d) silver nanoparticles under the optimized conditions (5 mL extract, 3 mM AgNO_3 , pH 8 and 60 °C. (e, f, g) formation of gold nanoparticles under 2, 5 and 10 mL plant extract and (h) under the optimized conditions (pH = 8, 50 C and 20 min) at 2 mM gold solution

Figure 2

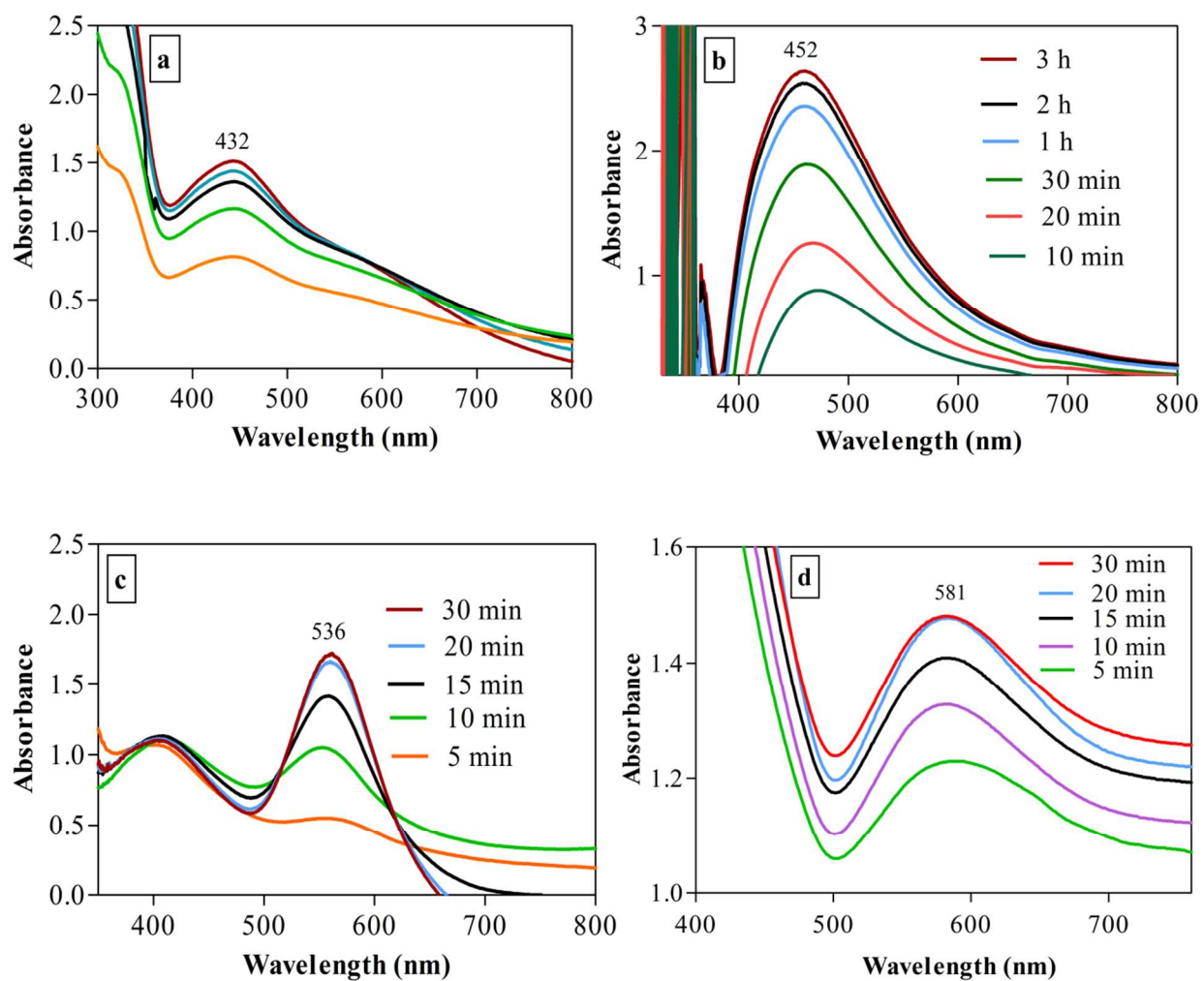


Fig. 2. UV-Vis spectra of silver and gold nanoparticles under varying amount of silver and gold ions keeping the plant concentration constant (5 mL), (a, b) Silver nanoparticles at 2 and 4 mM AgNO_3 . (c, d) gold nanoparticles at 1 and 3 mM gold solution

Figure 3

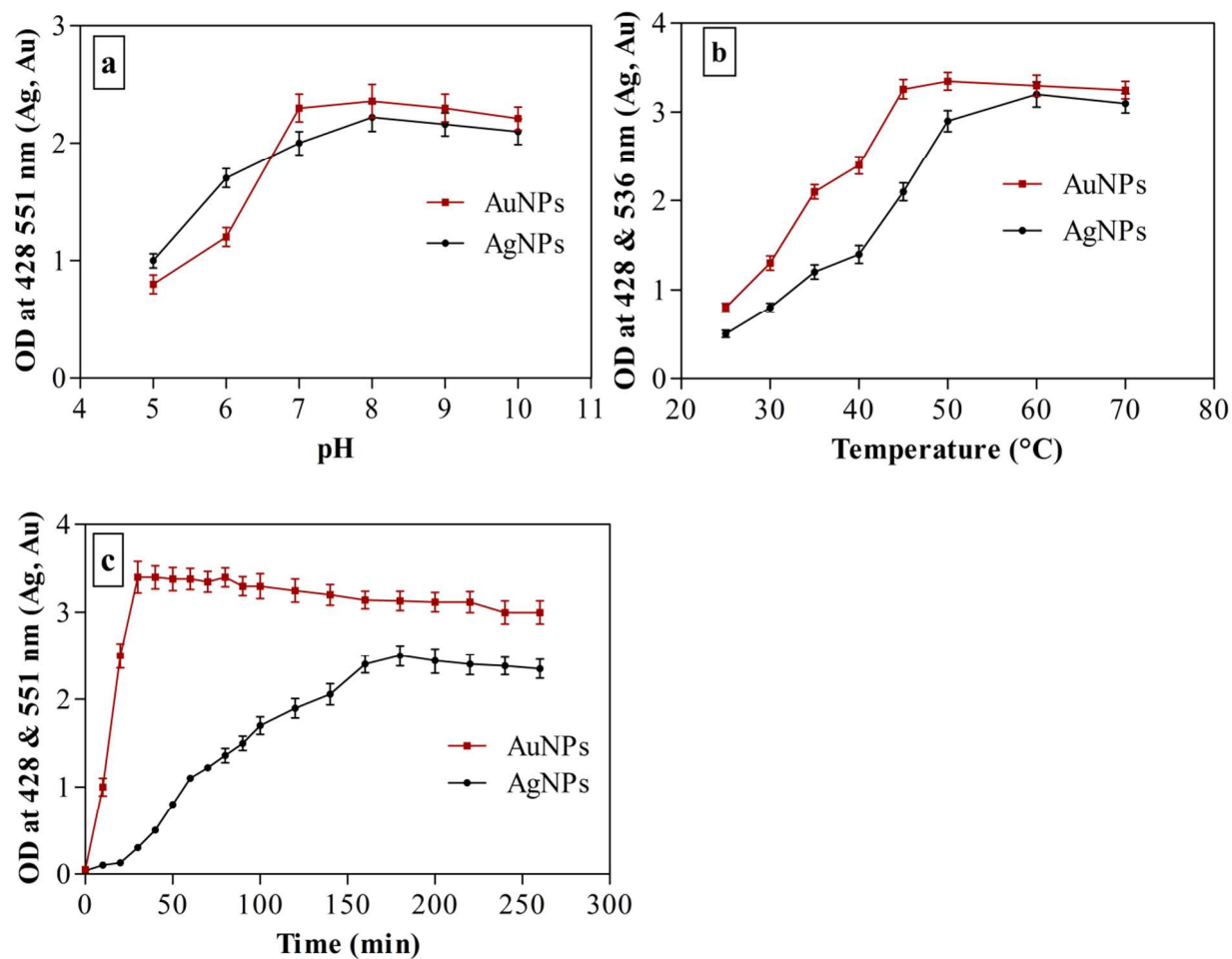


Fig. 3. Optimization of various parameters for the synthesis of silver and gold nanoparticles (a) pH (b) temperature and (c) time

Figure 4

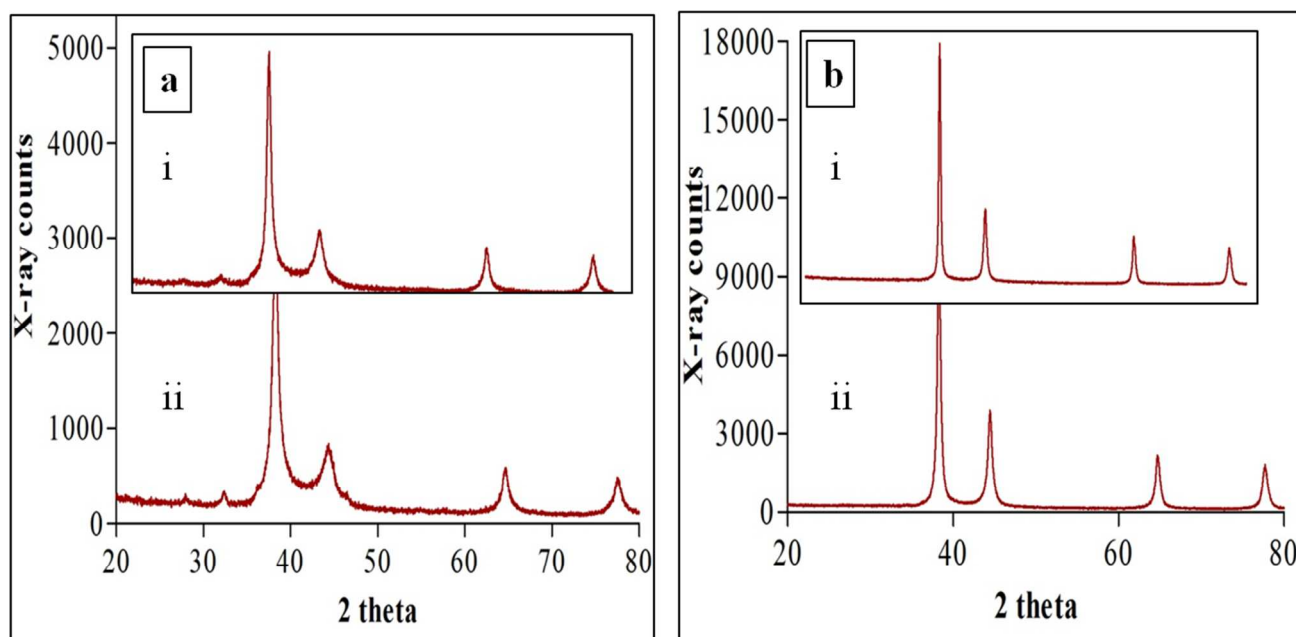


Fig. 4. X-ray diffractogram of silver and gold nanoparticles. (a) XRD pattern of silver nanoparticles of different sizes as evident from the comparative broadening of the representative peaks, (i) comparatively narrow than (ii) (b) Represents the comparative XRD pattern of gold nanoparticles of different sizes, (i) larger particles with narrow peaks and (ii) comparatively broader peaks indicating small particles size

Figure 5

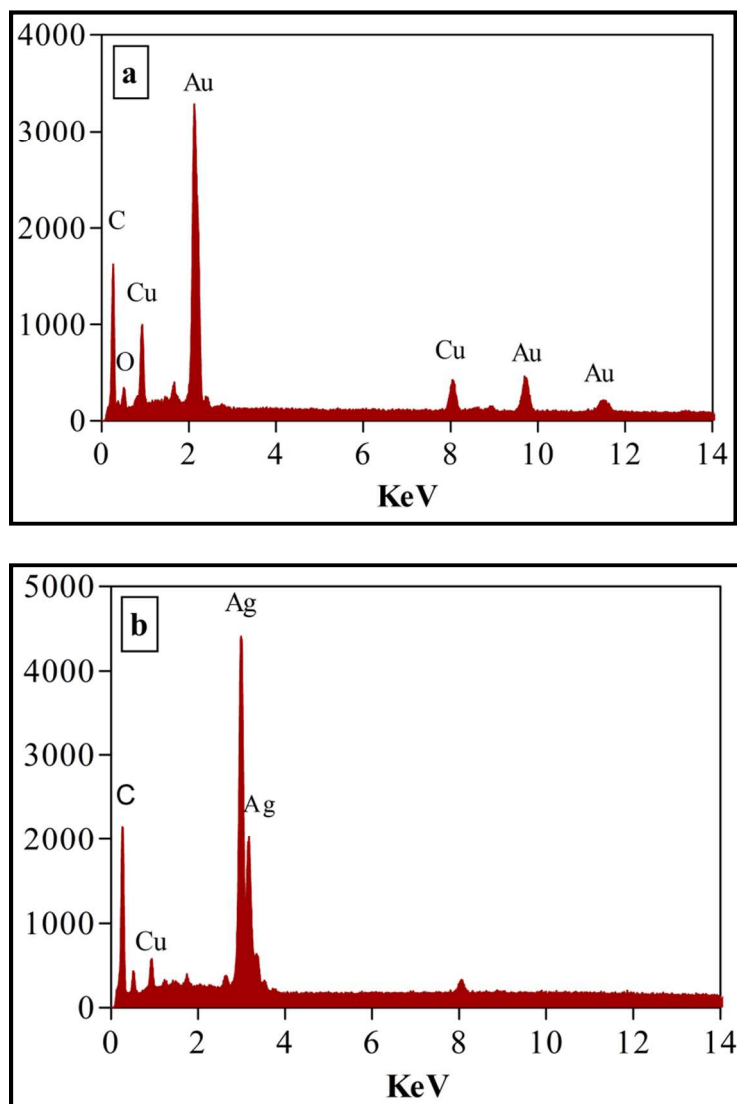


Fig. 5. EDX analysis of silver and gold nanoparticles (a) EDX pattern of nanoparticles confirming the presence of elemental silver as major constituent, (b) EDX pattern of gold nanoparticles, showing gold signal as major peak

Figure 6

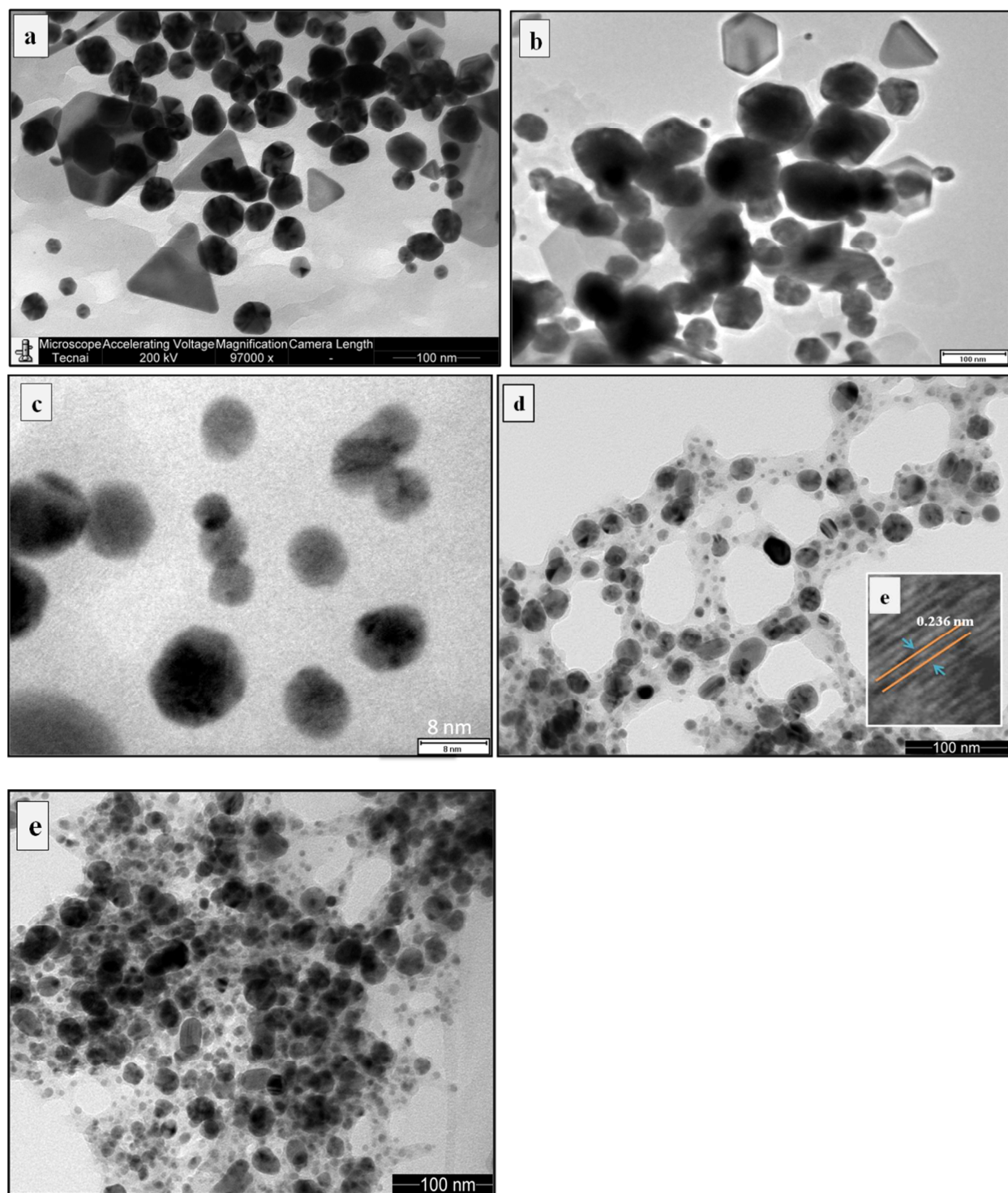


Fig. 6. (a) HRTEM image of gold nanoparticles synthesized at 5 mL plant extract (3mM (HAuCl₄.4H₂O)). (b) Gold nanoparticles synthesized at 12 mL plant extract. (c,d) AgNPs

synthesized at 5 and 12 mL plant extract (3 mM AgNO₃). (e) AgNPs synthesized with aqueous extract after tannin precipitation with polyvinyl polypyrrolidone (PVPP).

Figure 7

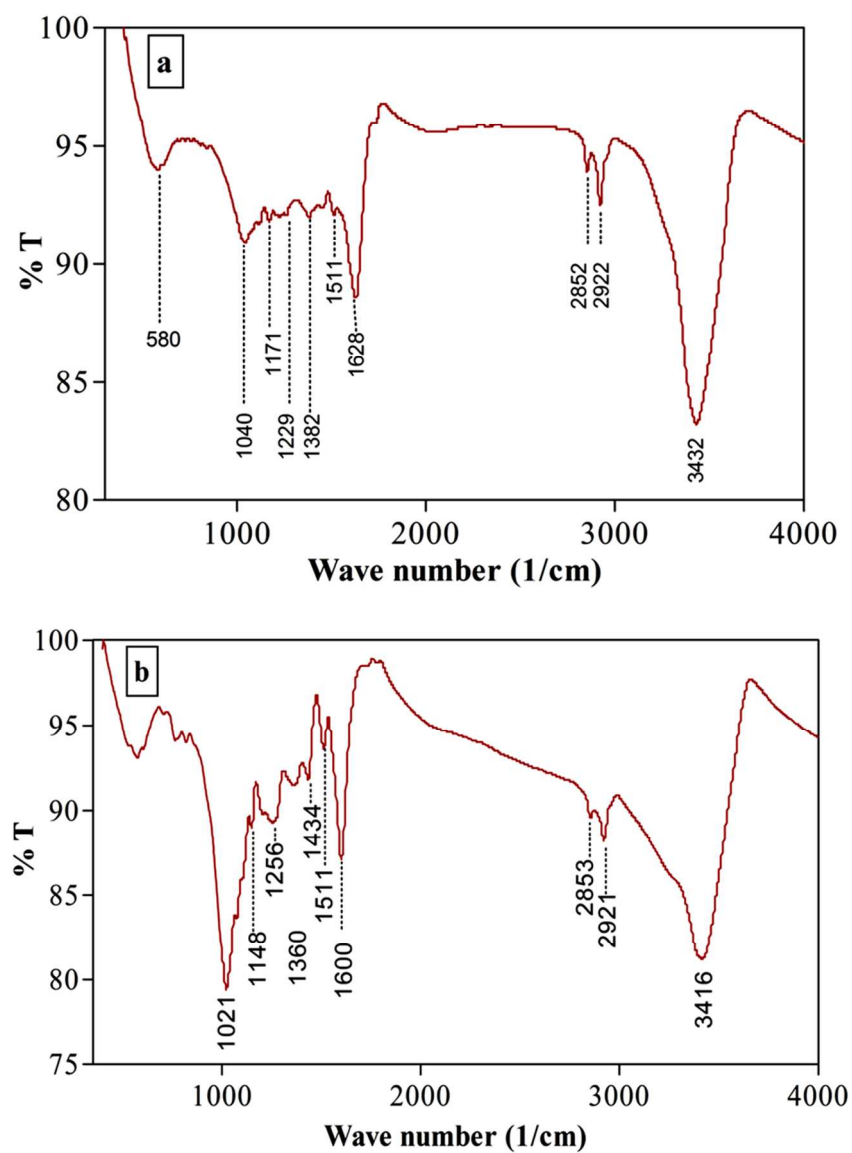


Fig. 7. FTIR spectra of (a) *Sargentodoxa cuneata* mediated synthesis of silver and (b) gold nanoparticles

Figure 8

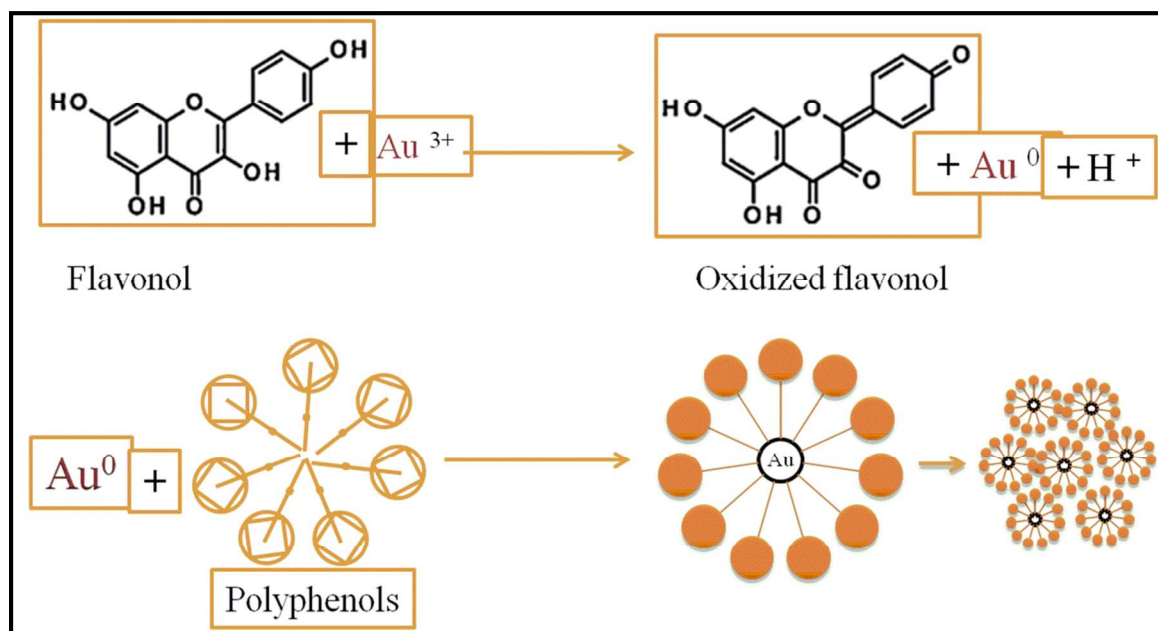


Fig. 8. Possible mechanism involved in the phytosynthesis of gold nanoparticles

Figure 9

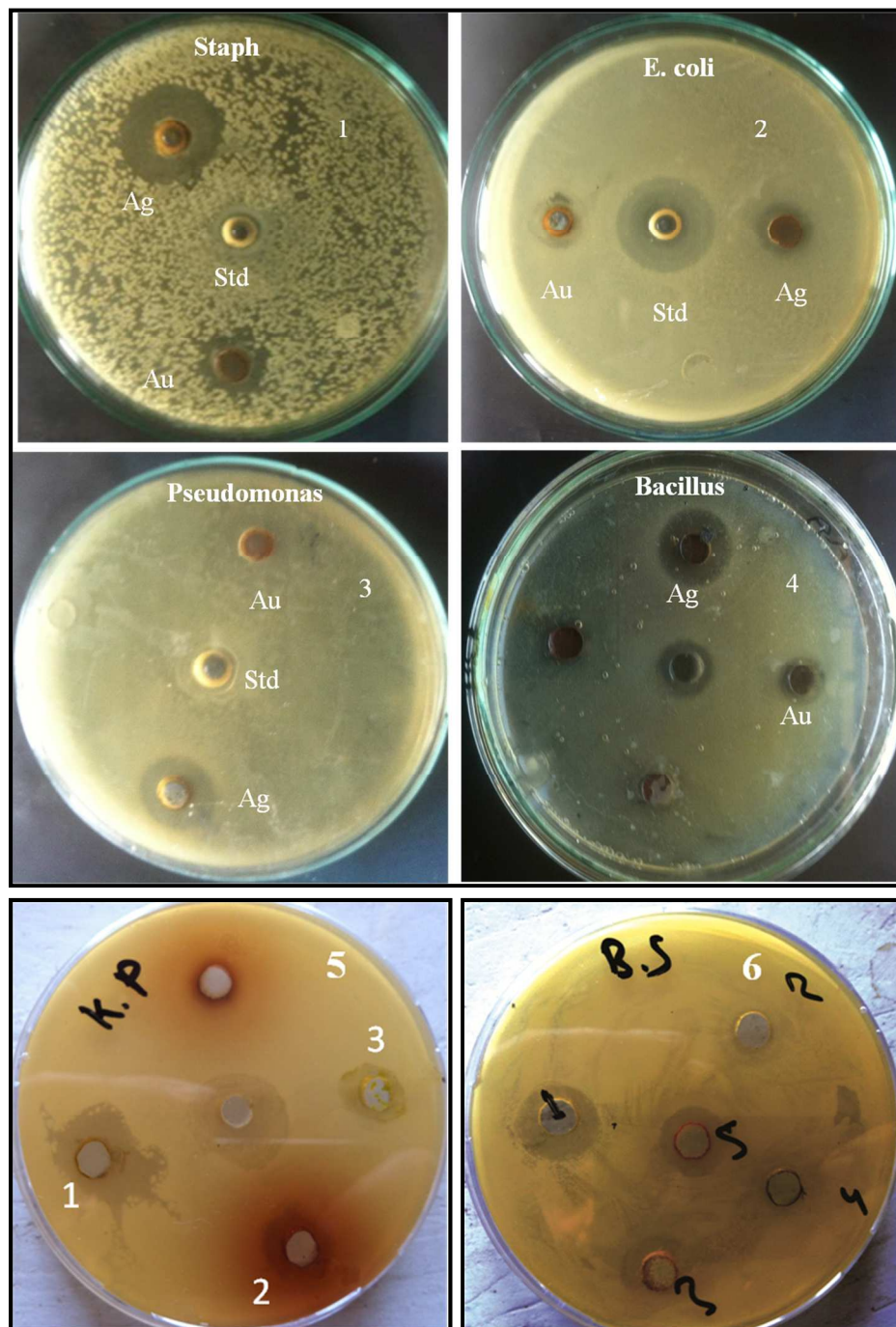
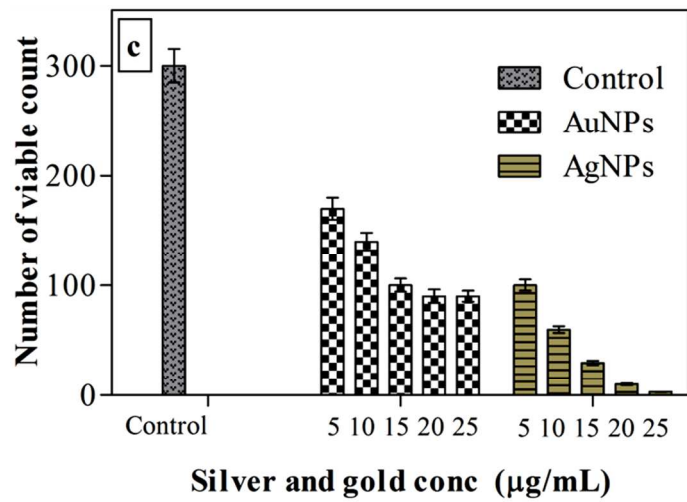
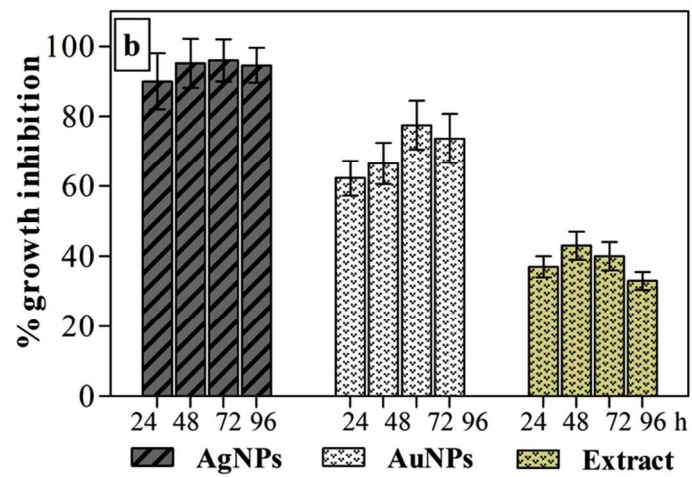
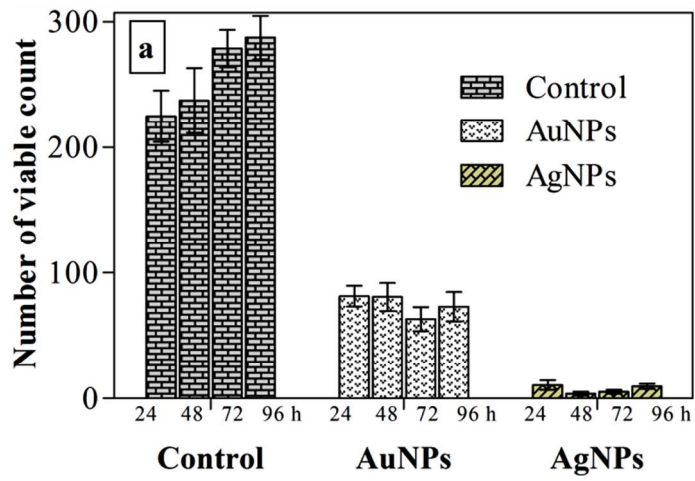


Fig. 9. Antibacterial activity (1-4) of *Sargentodoxa cuneata* mediated silver and gold nanoparticles against *Staphylococcus aureus*, *E. coli*, *Pseudomonas aeruginosa*, and *Bacillus subtilis*. (5,6) Comparative antibacterial activities of *Sargentodoxa cuneata* mediated (1) and

chemically synthesized (3) silver nanoparticles against *Klebsiella pneumoneae* and *Bacillus subtilis* respectively.

Figures 10



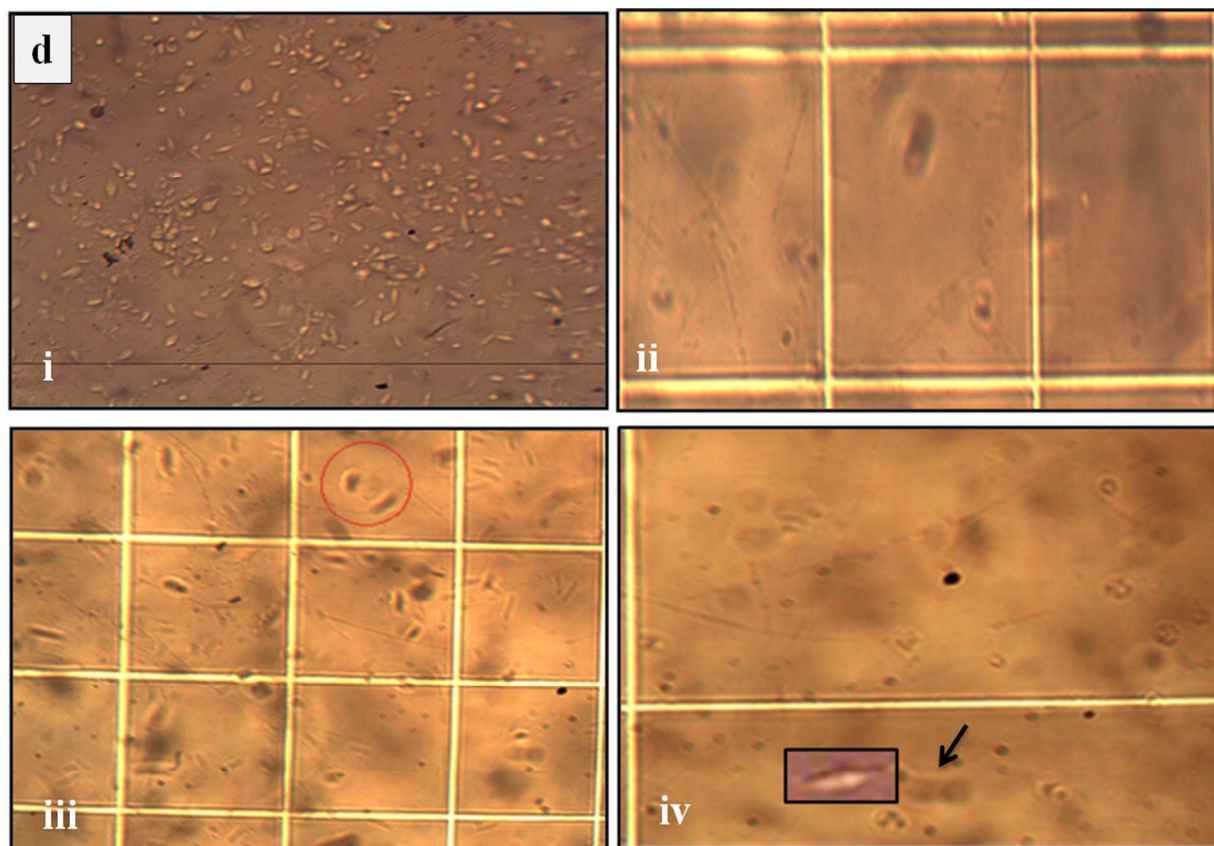


Fig. 10. Antileishmanial activity of silver and gold nanoparticles (a) Number of viable cells count in control and treated samples at different time intervals. (b) % growth inhibition of *Leishmania tropica* after exposure to silver and gold nanoparticles and (c) dose dependent antileishmanial activities of silver and gold nanoparticles. (d) Microscopic view of parasites (i) in the control group (not exposed to silver nanoparticles (ii) in the group exposed to silver nanoparticles in the dark, and (iii) in the group exposed to gold nanoparticles in the dark for 24 h and (iv) showing the distorted morphology of leishmania.

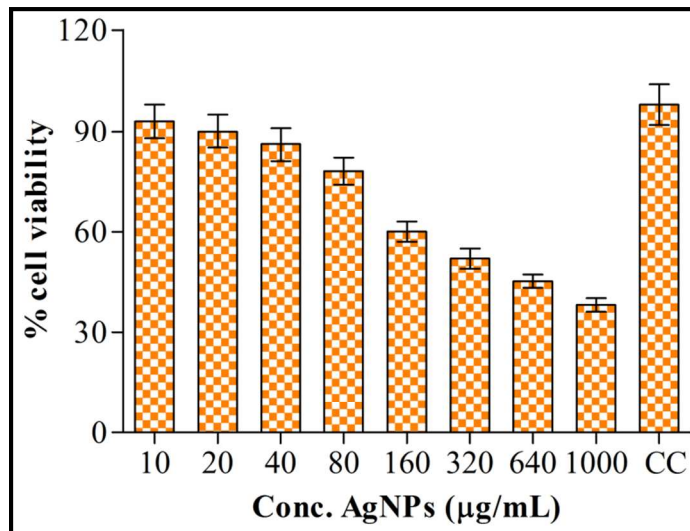
Figure 11

Fig. 11. Dose dependent cytotoxicity of *Sargentodoxa cuneata* mediated silver nanoparticles against murine macrophages. Results are expressed as a mean with bars showing mean \pm SD, CC, control group.

Table 1. Phytochemical screening of aqueous extract of *Sargentodoxa cuneata*

Phytochemicals	Inference
Alkaloids	+
Flavonoids	+
Terpenoids	+
Tannins	+
Saponins	+
Glycosides	+

Table 2. Antibacterial activity of silver and gold nanoparticles

<i>Bacteria</i>	AgNPs	AuNPs	Streptomycin
		Zone of inhibition (mm)	
<i>Staphylococcus aureus</i>	32 ± 2.6	12 ± 0.8	00
<i>Pseudomonas aruginosis</i>	16 ± 2	08 ± 0.5	00
<i>Bacillus subtilis</i>	18 ± 2	06 ± 0.5	08 ± 0.6
<i>E. coli</i>	12 ± 1	11 ± 1	21 ± 2.2